Title

Mitochondria-encoded genes contribute to evolution of heat and cold tolerance in yeast

Authors

Xueying C. Li[1,2,3], David Peris[4,5], Chris Todd Hittinger[4], Elaine A. Sia[6], Justin C. Fay[2,3,6,*]

Affiliations

[1]Molecular Genetics and Genomics Program, Division of Biology and Biomedical Sciences, Washington University, St. Louis, MO 63110, USA.

[2]Department of Genetics, Washington University, St. Louis, MO 63110, USA.

[3]Center for Genome Sciences and System Biology, Washington University, St. Louis, MO 63110, USA.

[4]Laboratory of Genetics, DOE Great Lakes Bioenergy Research Center, Genome Center of Wisconsin, Wisconsin Energy Institute, J. F. Crow Institute for the Study of Evolution, University of Wisconsin–Madison, Madison, WI 53706, USA.

[5]Department of Food Biotechnology, Institute of Agrochemistry and Food Technology (IATA), CSIC, Paterna, Valencia, Spain.

[6]Department of Biology, University of Rochester, Rochester, NY 14627, USA.

*Correspondence to: Justin C. Fay (justin.fay@rochester.edu).

Abstract

Genetic analysis of phenotypic differences between species is typically limited to interfertile species. Here, we conduct a genome-wide non-complementation screen to identify genes that contribute to a major difference in thermal growth profile between two reproductively isolated yeast species, *Saccharomyces cerevisiae* and *S. uvarum*. The screen revealed a single nuclear-encoded gene, but a large effect of mitochondrial DNA (mitotype) on both heat and cold tolerance. Recombinant mitotypes indicate multiple genes contribute to thermal divergence and we show that protein divergence in *COX1* affects both heat and cold tolerance. Our results point to the yeast mitochondrial genome as an evolutionary hotspot for thermal divergence.

One Sentence Summary

The mitochondrial genome is a hotspot for divergence in thermal growth differences in yeast.

MAIN TEXT

Introduction

The genetic architecture of phenotypic divergence between species is unresolved. There remains considerable uncertainty as to whether evolution occurred through accumulation of numerous small-effect changes ("micromutationism") or often involves "major genes" of large effect (*1*). While quantitative trait mapping has been successfully applied to closely related, interfertile species (reviewed in (*2*)), the results may not be representative of phenotypic divergence in general, since the characters that distinguish sibling species and domesticated organisms evolved over short time-scales and potentially favor large-effect loci. However, systematic dissection of divergence between distantly related species has been difficult due to reproductive barriers.

The *Saccharomyces* lineage contains post-zygotically isolated species with substantially diverged genomes, and the ease of genetic manipulation of yeast may allow us to address the genetic architecture of evolution with a systematic approach. While the *Saccharomyces* yeast species share their preference for fermentative metabolism with many other yeast species (*3*), they differ dramatically in their thermal growth profile (*4*, *5*). *S. cerevisiae* is the most heat-tolerant species in this lineage, capable of growing at temperatures of 37-42°C, while its sister species *S. paradoxus* can grow up to 39°C and the more distantly related *S. kudriavzevii* and *S. uvarum* are more cold-tolerant and only capable of growing at temperatures up to 34-35°C (*4*, *5*). Previous studies in yeasts have implicated a small number of genes involved in temperature divergence (*4*, *6*). However, every gene product has the potential to be thermolabile, and only a single systematic screen has been conducted (*7*), which reported that multiple genes contribute to thermal differences between *S. cerevisiae* and *S. paradoxus*, two species with modest differences in heat tolerance.

In the present study, we examined the genetic basis of thermal divergence between *S. cerevisiae* and *S. uvarum*, two species that are more different at synonymous sites than human and mouse (*8*, *9*). These two species are capable of forming hybrids, but the hybrids cannot produce viable spores. Mechanisms underlying the reproductive isolation could involve mitochondrial-nuclear incompatibilities (*10*, *11*), defects in recombination due to high levels of sequence divergence (*12*, *13*) and chromosomal rearrangements (*14*, *15*). Of relevance, mitochondrial genome variation has been shown to impact high temperature growth in *S. cerevisiae* (*16*, *17*) and *S. paradoxus* (*18*).

To identify genes involved in the evolution of thermal growth differences, we screened 4,792 non-essential genes for non-complementation and used the reciprocal hemizygosity test (*19*) to validate genes that came out of the screen. While no single genes of large effect were recovered, we found that mitochondrial DNA (mtDNA) plays a remarkable role in divergence of both heat and cold tolerance across the *Saccharomyces* species and that multiple mitochondria-encoded genes are involved, including *COX1*, previously shown to be involved in mitochondrial-nuclear interspecific incompatibilities (*11*).

Results

A non-complementation screen for thermosensitive alleles reveals mitochondrial effects

Hybrids of *S. cerevisiae* and *S. uvarum* are heat tolerant (Fig. 1A). Thus, deletion of *S. cerevisiae* heat tolerant alleles in a hybrid should weaken heat tolerance through non-complementation. We screened 4,792 non-essential genes in the yeast deletion collection for such thermotolerance genes by mating both the *MAT***a** (BY4741) and *MAT*α (BY4742) deletion collection to *S. uvarum* and growing them at high temperature (37°C). For comparison, we also screened the resulting hemizygote collections for two other traits where the *S. cerevisiae* phenotype is dominant in the hybrid (Fig. 1A): copper resistance (0.5 mM copper sulfate) and ethanol resistance (10% ethanol at 30°C). We found 80, 13, and 2 hemizygotes that exhibited reduced resistance to heat, copper, and ethanol, respectively, in both the BY4741 and BY4742 hemizygote collections (Fig. 1B). In our initial assessment of these genes, we validated a copper-binding transcription factor, *CUP2* (*20*), for copper resistance through reciprocal hemizygosity analysis (Fig. S1).

Nearly all of the heat-sensitive hemizygotes (77/80) were from respiration-deficient ("petite") *S. cerevisiae* parents. We found many of these strains carried *S. uvarum* mitochondrial DNA (mtDNA) via PCR of a mitochondrial marker. Although not extensively tested, other hemizygotes are expected to carry *S. cerevisiae* mtDNA, a typical outcome of *S. cerevisiae* × *S. uvarum* crosses (*21*). The difference in mtDNA inheritance was likely caused by loss of mtDNA in the *S. cerevisiae* petite parents. We confirmed one gene (*HFA1*) by reciprocal hemizygosity analysis (Fig. 1C, Fig. S1) that causes a moderate loss of heat tolerance due to the *S. uvarum* allele in the presence of *S. cerevisiae* mtDNA. *HFA1* encodes a mitochondrial acetyl-coenzyme A carboxylase and is involved in mitochondrial fatty acid biosynthesis (*22*).

The inheritance of *S. uvarum* mtDNA in heat-sensitive hemizygotes suggested that mtDNA, rather than the deletion, could be the cause. To test whether the species' mtDNA ("mitotype") affects heat tolerance, we generated diploid hybrids of wild-type *S. cerevisiae* and *S. uvarum* with reciprocal mitotypes and grew them at different temperatures. In comparison to the hybrid with *S. cerevisiae* mitotype, the hybrid with the *S. uvarum* mitotype showed reduced fermentative growth (glucose medium) at 37°C compared to 22°C and almost no respiratory growth (glycerol medium) at 37°C (Fig. 2A).

S. uvarum is not only known to be heat sensitive, but also exhibits enhanced growth at low temperatures relative to *S. cerevisiae* (*4*). We thus tested and found that *S. uvarum* mitotype conferred a growth advantage at 4°C in comparison to *S. cerevisiae* mitotype (Fig. 2A), suggesting a potential trade-off between the evolution of heat and cold tolerance.

To test whether mtDNA-mediated evolution of temperature tolerance is specific to either the *S. cerevisiae* or *S. uvarum* lineages, we generated five additional hybrids with both parental mitotypes using two other *Saccharomyces* species (Fig. S2). In comparison to the 22°C control, we find that both the *S. cerevisiae* and *S. paradoxus* nuclear genome conferred heat tolerance to hybrids with *S. kudriavzevii* and *S. uvarum* (rho^o comparison), but the *S. cerevisiae* mitotype conferred heat tolerance in comparison to the *S. paradoxus, S. kudriavzevii,* and *S. uvarum* mitotypes on glucose medium. For cold tolerance we find that the *S. uvarum* mitotype conferred greater cold tolerance relative to the *S. cerevisiae, S. paradoxus,* and *S. kudriavzevii* mitotypes. Interestingly, none of the hybrids was as cold tolerant as *S. uvarum* on glycerol. Our results suggest that mtDNA has played an

important role in divergence of thermal growth profiles among the *Saccharomyces* species, with heat tolerance evolving primarily on the lineage leading to *S. cerevisiae* and cold tolerance evolving primarily on the lineage leading to *S. uvarum*. A related study has shown these differences have had a direct impact on the domestication of lager-brewing yeast hybrids to low-temperature fermentation (*23*).

Recombinant analysis identifies contribution of multiple mitochondria-encoded genes

To identify mtDNA genes conferring heat tolerance to *S. cerevisiae*, we tested whether *S. uvarum* alleles can rescue the respiratory deficiency of *S. cerevisiae* mitochondrial gene knockouts at high temperature. We crossed *S. uvarum* to previously constructed *S. cerevisiae* mitochondrial knockout strains and plated them on glycerol medium at 37°C. Because heteroplasmy is unstable in yeast, this strategy selects for recombinants between the two mitochondrial genomes: *S. uvarum* mtDNA is needed to rescue the *S. cerevisiae* deficiency, and *S. cerevisiae* mtDNA is needed to grow at high temperature (Fig. S3). If the *S. uvarum* gene required for *S. cerevisiae* rescue is temperature sensitive, we expect to see no or small colonies on 37°C glycerol plates. Of the six genes tested, *COX2* and *COX3* deletions were rescued by *S. uvarum* at high temperature, although the colonies were often smaller than the hybrid with wild-type *S. cerevisiae* mtDNA. In contrast, *COX1* and *ATP6* deletions were minimally rescued (Fig. 2B), and *COB* and *ATP8* deletions were not rescued. However, the absence of rescue could also result from a lack of recombination, especially for *COB* because its genomic location has moved between the two species.

Using genome sequencing, we mapped breakpoints in 90 recombinants to determine which *S. cerevisiae* genes are associated with high temperature growth. The recombinants showed hotspots at gene boundaries and within the 21S ribosomal RNA (Fig. 2B). In most cases, the two species' mtDNA recombine into a circular mitochondrial genome, but sometimes recombination resulted in mitochondrial aneuploidy, particularly for regions where the two species' mitochondrial genomes are not co-linear (see Fig. S4B for examples). One complication of measuring mtDNA-dependent heat tolerance is the high rate of mtDNA loss, typically 1% in *S. cerevisiae* strains, but much higher in the hybrids and variable among recombinants (Supplementary text, Fig. S5). We thus measured the frequency of petites at 22°C and heat tolerance by the size of single colonies at 37°C on glycerol. We found that the petite frequency was associated with the absence of *S. cerevisiae ORF1* (F-*Sce*III, (*24*), a homing endonuclease linked to *COX2* (Fig. S5B & C). For heat tolerance, we found a region including four protein-coding genes (*COX1*, *ATP8*, *ATP6*, and *COB*) with the largest effect (Fig. 2C). The effects associated with these genes are small compared to the total difference between two wild-type mitotypes, suggesting that other regions are required for complete rescue of high temperature growth. Indeed, *S. cerevisiae COX2* and *COX3* showed small but positive effects when the recombinants lacking them were compared to the wild-type *S. cerevisiae* mitotype (Fig. 2B). The differential heat sensitivity is unlikely to be caused by fitness defects since the recombinants grew normally at 22°C (Fig. S4A).

We also found that nearly all mtDNA recombinants did not exhibit 4°C respiratory growth; one strain (S87) derived from the *atp6Δ* cross (Figure 2B) was an exception, but another strain with the same mitochondrial genotype did not grow. The 4°C recombinant

phenotypes suggest that cold tolerance might require multiple *S. uvarum* alleles and potentially a different set of genes than those underlying heat tolerance.

COX1 protein divergence affects both thermotolerance and cryotolerance

Because the recombinant strains did not resolve heat tolerance to a single gene, we tested individual genes by replacing *S. cerevisiae* with *S. uvarum* alleles via biolistic transformation (*25*) (Fig. S6). We obtained allele replacements for two of the four genes in the region conferring heat tolerance (Fig. 3). For both genes we used intronless alleles to eliminate incompatibilities in splicing (*11*).

We observed a significant difference between *S. cerevisiae* and *S. uvarum COX1* alleles for respiratory growth at 37°C in the hybrid background, with the *S. uvarum* allele being heat sensitive. The effect was not present at room temperature, and the *S. uvarum* allele conferred a growth advantage on glucose at 4°C. Thus, divergence in the *COX1* coding sequence (CDS) affects both heat and cold tolerance. However, *COX1* alleles do not explain the entire difference between the two species' mitotypes: the strain bearing *S. uvarum COX1* had an intermediate level of heat tolerance and did not confer cold tolerance on glycerol, suggesting that other mitochondrial genes are involved. The moderate effect of the *COX1* alleles is also consistent with the small effect sizes shown by recombinant analysis (Fig. 2C). Surprisingly, the *COX1* allele difference is only seen in the hybrid and not in a diploid *S. cerevisiae* background (Fig. S7), suggesting that the allele difference in the hybrid depends on a dominant interaction with the *S. uvarum* nuclear genome.

The *S. uvarum COB* allele replacement rescued respiratory growth at high temperature, demonstrating that the *S. uvarum COB* protein is not heat sensitive. We were unable to generate the *S. cerevisiae* intronless *COB* allele replacement for comparison. Notably, both the intronless *S. cerevisiae COX1* and *S. uvarum COB* allele replacement strains exhibited better growth than wild-type *S. cerevisiae* mtDNA at 37°C (Fig. 3), implying a dominant-negative role of these introns in the hybrid at high temperature.

Discussion

In *Saccharomyces* species, the mitochondrial genome is not essential for viability, is large compared to insects and mammals (~86 kb), and is quite variable in intron content (*26*). While the mitochondrial genome can recombine and introgress between species (*18*, *24*), it also contributes to reproductive isolation through incompatibilities with the nuclear genome (*10, 11, 27*). Our results show that the mitochondrial genome also makes a significant contribution to one of the most distinct phenotypic differences among the *Saccharomyces* species: their thermal growth profile. Below, we discuss the implications of our results in relationship to the genetic architecture of species' phenotypic differences, the role of cyto-nuclear interactions in phenotypic evolution and reproductive isolation, and mitochondria as a hotspot in the evolution of *Saccharomyces* species.

Genetic architecture of interspecies differences in thermotolerance

Crosses between closely related, inter-fertile species have shown that phenotypic divergence can be caused by a few loci of large effect, many loci of small effect or a

mixture of the two (*2*). In this study, we carried out a genome-wide non-complementation screen between two diverged yeast species. Out of 4,792 non-essential genes in our study, we found only one gene (*HFA1*) that showed a moderate effect on heat tolerance regardless of the mtDNA effect (Fig. 1C). Of relevance, 178 *S. cerevisiae* deletions are sensitive to 37°C (*28*); a rate comparable to a subsample we examined in this study (78/2251). We can thus conclude that the vast majority of the *S. uvarum* alleles tested exhibited no detectable loss of function at a temperature they do not experience in their native genome. However, our non-complementation screen had some limitations. We did not test essential genes and could not detect genes whose effects were masked by mtDNA inheritance or epistasis, which could occur due to the hybrid carrying an otherwise complete complement of both nuclear genomes.

We found allele differences in *HFA1* affect heat tolerance. *HFA1* encodes a mitochondrial acetyl-CoA carboxylase and participates in mitochondrial fatty acid synthesis, a process essential to cellular respiration and mitochondrial biogenesis (*29*). While disruption of *HFA1* in *S. cerevisiae* resulted in a low level of lipoic acid and consequently a temperature-dependent respiratory defect (*22*, *30*), the hemizygote with only the *S. uvarum* allele showed heat sensitive growth on glucose but not glycerol (Fig. S1C), suggesting that the divergence in heat tolerance of *HFA1* might not be directly linked to its role in respiration. Further investigation is needed to elucidate the molecular mechanism by which *HFA1* impacts thermal divergence.

Although our screen led us to discover a pronounced temperature dependent effect of mtDNA on respiratory growth and a more subtle effect on fermentative growth, the mtDNA effect explains only a small portion of the large difference in heat tolerance between the two species. The *S. cerevisiae* × *S. uvarum* hybrid without mtDNA grows at both 37°C and 4°C on glucose (Fig. 2B), indicating that the nuclear genomes carry dominant factors that remain to be identified.

Despite the small number of genes in the mitochondrial genome, our results show multiple genes within the mitochondrial genome influence heat tolerance. In addition to the large effect of the *COX1-COB* region, recombinants that inherited *S. uvarum COX2* and/or *COX3* are considerably more heat sensitive than a hybrid with a complete *S. cerevisiae* mtDNA genome. Furthermore, while the *COX1*-linked region showed the largest effect, the *COX1* CDS does not explain the entire difference between two species' mitotypes. Although we ruled out protein-coding changes in *S. uvarum COB* to be heat sensitive, changes in the other protein-coding sequences and in gene expression remain to be tested.

The cause of mtDNA-mediated differences in cryotolerance is more opaque. At 4°C, only one recombinant with a significant fraction of *S. cerevisiae* mtDNA grew better than hybrids with an *S. cerevisiae* mitotype, suggesting that multiple *S. uvarum* alleles are required for cold tolerance. Although we showed that *S. uvarum COX1* increased cold tolerance on glucose, the effect is not seen on glycerol, suggesting its effect on respiration might depend on the presence of other *S. uvarum* mitochondrial alleles. However, because the recombinants were all isolated at 37°C, it is possible that they all share some other genetic element or change that facilitates heat tolerance but inhibits 4°C growth.

Cyto-nuclear interactions in Saccharomyces evolution

In addition to mitochondria-encoded genes, approximately 1,000 nuclear genes function in the mitochondria, many of which are involved in expression and regulation of mitochondrial genes and formation of the multi-subunit cytochrome b and c complexes (*31*). Among *Saccharomyces* species, multiple cyto-nuclear incompatibilities have been shown to contribute to reproductive isolation. *S. uvarum AEP2* cannot regulate the translation of *S. cerevisiae ATP9* mRNA (*10*), while *S. cerevisiae MRS1* cannot splice introns of *S. paradoxus* and *S. uvarum COX1* (*11*). Additionally, the *S. uvarum* RNA binding protein *CCM1* has reduced affinity for the *S. cerevisiae* 15s rRNA (*32*). While these incompatibilities affect the construction of cybrids, where mtDNA from different species was introduced into *S. cerevisiae* (*27*), the phenotypic consequences besides loss of respiration is not known.

Our results show that the mitochondrial genomes of *Saccharomyces* species influence both heat and cold tolerance and provide multiple lines of evidence for the role of cyto-nuclear interactions. First, the temperature effects of species' mitotypes interact with nuclear background (Fig. S1). While *S. cerevisiae* hybrids without mtDNA (rho^o) grow similarly on glucose medium, *S. cerevisiae* mtDNA confers different levels of heat tolerance in hybrids with *S. paradoxus*, *S. uvarum*, and *S. kudriavzevii*, the latter of which only grows slightly better than the rho^o hybrid.

We also observed interactions between the *COX1* allele replacements and their nuclear background. *COX1* showed allele differences at high and low temperatures in the hybrid but not in *S. cerevisiae*. This difference can be explained by a species-specific dominant interaction, as might occur when there are hybrid protein complexes (*33*). In this scenario, *S. uvarum COX1* can function with interacting *S. cerevisiae* proteins at high temperature but exhibits a loss of function when interacting with temperature sensitive *S. uvarum* nuclear factors that are dominant to their *S. cerevisiae* orthologs. The nuclear factor is unlikely to be the previously reported intron-splicing factor *MRS1* because our *COX1* alleles are intronless.

However, introns might affect temperature sensitivity. The intronless *S. cerevisiae COX1* and *S. uvarum COB* alleles showed better respiratory growth at 37°C than wild-type *S. cerevisiae* mtDNA, suggesting a dominant negative role of introns in the hybrid. In *Saccharomyces*, the number and presence of mitochondrial introns is variable between species (*34*). This contrasts with high conservation of mitochondrial protein coding sequences, which show over 90% sequence identity between *S. cerevisiae* and *S. uvarum*, much higher than the 80% average of nuclear-encoded genes (*35*). The rapid evolution of introns might require co-evolution of splicing factors, such as *COX1* and *MRS1*. The wild-type hybrid with *S. cerevisiae* mtDNA might be under burden of intron splicing at high temperature caused by dominant negative *S. uvarum* splicing factors. Nevertheless, many introns self-splice and/or encode maturases or homing-endonucleases, which could be temperature sensitive in a nuclear-independent manner.

There is no clear indication that previously reported incompatibilities contribute to the mtDNA temperature phenotypes. The reported cyto-nuclear incompatibilities are recessive, and thus should not contribute to the hybrid phenotypes. For example, although the *S. cerevisiae MRS1* is incompatible with *S. uvarum COX1*, the latter can be correctly spliced by *S. uvarum MRS1* in the diploid hybrid, at least at permissive temperatures. One possibility is that *S. uvarum MRS1* is heat sensitive, which would explain the heat

sensitivity of the *S. uvarum* mitotype because neither the *S. cerevisiae* nor *S. uvarum* *MRS1* would splice *S. uvarum COX1* at high temperature. Heat sensitivity of *S. uvarum* *MRS1* was tested in our non-complementation screen, but the result was inconclusive. The *S. cerevisiae MRS1* deletion was complemented by the *S. uvarum* allele in the *MAT***a** (BY4741) cross; but its effect was masked by mtDNA inheritance in the *MAT*α (BY4742) cross. In this regard it is worth noting that *S. cerevisiae* chromosome 9, which carries *MRS1*, is duplicated in three of the recombinant strains; in two cases, these strains show increased 37°C growth compared to similar genotypes (Table S1).

Mitochondrial DNA and yeast evolution

It has been proposed that mtDNA plays a disproportionate role in Dobzhansky-Muller incompatibilities. Although it is a small genome, it heavily interacts with nuclear genes and has a high nucleotide substitution rate, leading to co-evolution of the mitochondrial and nuclear genomes and multiple interspecific incompatibilities (*36*). Has adaptation played a role in driving these incompatibilities? Although no direct links are proven, evolution of the mitochondrial genome and mito-nuclear epistasis has been linked to multiple phenotypes (*21*, *37*, *38*), including 37°C growth (*16*–*18*), and deficiencies in mitochondrial DNA cause heat sensitivity (*39*). Here, we show that mtDNA is important for evolution of heat and cold tolerance in distantly related species, caused by the accumulation of multiple small-to-medium effect changes and potentially mito-nuclear epistasis. Taken together, the present and prior findings point to mtDNA as an evolutionary hotspot for yeast speciation and adaptation.

Materials and Methods

Strains, growth conditions, and genetic manipulations

Strains used in this study are listed in Table S2. *S. cerevisiae* was maintained on YPD (1% yeast extract, 2% peptone, 2% dextrose) at 30°C; *S. uvarum* and *S. cerevisiae* × *S. uvarum* hybrids were maintained on YPD at room temperature. Strains were also grown on complete medium (CM, 0.3% yeast nitrogen base with amino acids, 0.5% ammonium sulfate, 2% dextrose), or dropout medium (CM-xxx, 0.13% dropout powder, 0.17% yeast nitrogen base, 0.5% ammonium sulfate, 2% dextrose) where xxx represents the missing amino acids when appropriate. SDPSer medium (synthetic dextrose proline D-serine, 2% dextrose, 0.17% yeast nitrogen base without ammonium sulphate or amino acids, 5 mg/ml L-proline, 2 mg/ml D-serine) was used to select for *dsdAMX4* (*40*). Antibiotics were added to media when selecting for *KanMX*, *NatMX*, and *hphMX*. YPGly medium (1% yeast extract, 2% peptone, 3% glycerol) was used to examine respiratory growth.

S. cerevisiae and *S. uvarum* strains were mated by mixing strains with opposite mating types on YPD at room temperature overnight. Diploid hybrids were obtained by plating the mating mixture to double selection medium and confirmed by mating-type PCR.

Transformations in this study followed standard lithium acetate methods (*41*). When transforming *S. uvarum* or *S. cerevisiae* × *S. uvarum* hybrid, we used 37°C for heat shock and room temperature for incubation.

Strains lacking mitochondrial DNA (rho^0) were generated by overnight incubation with shaking in liquid minimal medium (MM, 0.17% yeast nitrogen base without amino

acid and ammonium sulfate, 0.5% ammonium sulfate, 2% dextrose) containing 25 ug/ml ethidium bromide. Following incubation, the culture was plated to YPD and YPGly to identify non-respiring colonies.

Interspecific hemizygote collections

trp1 S. uvarum strains YJF2600 and YJF2601 were constructed by replacing *TRP1* with *hphMX4* in YJF1449 (*MAT***a**) and YJF1450 (*MAT*α) in the CBS7001 background (*42*), respectively. The haploid yeast deletion collections derived from BY4741 (*MAT***a** *his3Δ1 leu2Δ0 met15Δ0 ura3Δ0*) and BY4742 (*MAT*α *his3Δ1 leu2Δ0 lys2Δ0 ura3Δ0*) were arrayed in 384-well format using a Singer ROTOR (Singer Instruments, Watchet UK) and mated to *trp1 S. uvarum* strains. Diploids were selected on CM-trp-his-leu-lys-ura plates. The resulting two interspecific hybrid collections were hemizygous for 4,792 genes.

The hemizygote collections were screened for non-complementation using the following conditions: 1) YPD at room temperature, 30°C, 35°C and 37°C; 2) CM with 0.5 mM copper sulfate at room temperature; and 3) YPD with 10% ethanol at 30°C. Pictures of plates were taken on the second and fifth day of incubation using a Nikon D3100 camera. Colonies that were visually smaller than wild-type (represented by most of the hemizygotes on the same plate) on day 5 were scored as sensitive, ranging from no growth to slightly sensitive growth. For heat, copper, and ethanol stresses, respectively, we found 145, 137, and 26 non-complemented genes from the BY4741 (*MAT***a**) cross and 221, 134, and 19 from the BY4742 (*MAT*α) cross, resulting in an intersection of 80, 13, and 2 genes (Data S1).

Respiration-deficient strains (petites) were identified by plating the haploid deletion collection strains on YPGly at 30°C. To estimate the rate of temperature-sensitive deletions, we sampled six plates (~2.3k strains) from the haploid deletion collections and assayed their growth on YPD plates at room temperature and 37°C. The rate of heat-sensitive deletions in the subsample was 78/2251.

Validation of non-complementing genes

We first repeated the non-complementation test in another strain background. We made deletions of candidate genes (*HFA1* for heat; *TDA1*, *TDA9*, *GGC1*, *TDA4*, *RPL39*, *ADD66*, *YOL075C*, *CUP2*, and *CAJ1* for copper) by *KanMX* in an *S. cerevisiae* strain YJF173 in the same way as the deletion collection, with the exception that the coding region of *HFA1* was defined according to (*30*). The knockout strains were then crossed to an *S. uvarum* rho^0 strain (YJF2760). Phenotypes of the hemizygotes were assessed at the same conditions as in the screen, and only phenotypes of *HFA1* and *CUP2* were replicated.

Reciprocal hemizygotes were generated for *HFA1* and *CUP2*. Orthologs of *S. cerevisiae HFA1* and *CUP2* were knocked out in *S. uvarum* strain YJF1450 with *KanMX*. The orthologs were defined according to (*42*); for *HFA1*, we included an extra 477 bp upstream of the ATG for the *S. uvarum* allele, based on translation from a non-AUG start codon at position -372 in *S. cerevisiae* (*30*). The *S. uvarum* deletion strains were then crossed to *S. cerevisiae* (YJF173), and the resulting hemizygotes were genotyped by PCR and found to carry *S. cerevisiae* mtDNA. Phenotypes of the two reciprocal hemizygotes were assessed on the same plate, under the same conditions as in the screen.

Interspecific hybrids with reciprocal mitotypes

Interspecific hybrids with reciprocal mitotypes were generated by crossing a rho$^+$ strain from one species to a rho^0 strain from another species. Two rho^0 colonies from each strain were crossed to control for possible mutagenic effects of the ethidium bromide treatment. Mitotype was confirmed by PCR using primers targeting the tRNA clusters in mtDNA (forward 5'-CCATGTTCAAATCATGGAGAGA-3', reverse 5'-CGAACTCGCATTCAATGTTTGG-3'; 95°C 2min; 95°C 30s, 50°C 30s, 72°C 30s for 30 cycles; 72°C 5min). The expected product sizes are 167 bp for *S. cerevisiae*, 131 bp for *S. paradoxus*, 218 bp for *S. kudriavzevii*, and 100 bp for *S. uvarum*.

Crosses with mitochondrial knockouts

S. uvarum strain YJF2600 (*MAT***a** *hoΔ::NatMX trp1Δ::hphMX4*) and YJF2601 (*MATα hoΔ::NatMX trp1Δ::hphMX4*) were crossed to previously constructed *S. cerevisiae* mitochondrial knockout strains (*43–48*). *S. cerevisiae* strains with wild-type mtDNA were crossed in parallel as control. *MAT***a** and *MATα* strains were mixed on YPD and incubated at room temperature overnight. The mating mixtures were either replica-plated (initial trial) or resuspended in sterile water and plated (second trial) onto YPGly. The YPGly plates were incubated at 37°C for 7-10 days to select for 37°C-respiring recombinants. The mating mixtures of *cox2Δ* and *cox3Δ* crosses were also plated to CM-trp-his-leu-lys-ura at room temperature to select for diploid hybrids, which allowed us to estimate the recombination rate to be around 0.05-0.1%. 37°C-respiring colonies were picked and streaked on YPD at room temperature for single colonies. For the initial trial, the 37°C-respiring cells were streaked on YPD twice. For the *cox1Δ* and *atp6Δ* crosses, the plates were left at room temperature for 3 days after 7 days at 37°C incubation and colonies growing from the recovery period were also picked and streaked. We also tried selecting for recombinants at 33°C and 35°C for the crosses with *cob*Δ, *atp6*Δ and *atp8*Δ strains, from which we isolated few recombinants at 37°C. However, selection at 35°C did not significantly increase either the number or the size of the recombinant colonies compared to 37°C, and 33°C is too low a temperature to distinguish any heat-tolerant recombinants from non-recombinant *S. uvarum* mtDNA; we thus did not sequence colonies from these selections. As a result, 3+12, 4+48, 3+25, 2+3, 0+7, and 0+1 strains (initial trial + second trial) from the *cox2Δ, cox3Δ, cox1Δ, cobΔ, atp6Δ* and wild-type D273-10B control crosses, respectively, were generated. The total of 102 strains were subjected to whole genome sequencing and phenotyping.

Spontaneous mitochondrial recombinants

S. cerevisiae (YJF153, *MAT***a** *hoΔ*::*dsdAMX4*, YPS163 derivative) and *S. uvarum* (YJF1450, *MATα hoΔ*::*NatMX*, CBS7001 derivative) were mated and streaked onto SDPSer + clonNAT medium to select for diploid hybrids. 384 colonies on the double selection plates were picked and arrayed onto one YPD agar plate and subsequently pinned to YPD and YPGly and incubated at room temperature, 37°C and 4°C. Colony sizes on each plate were scored both manually and quantitatively using ImageJ (*49*). Strains with recombinant-like temperature phenotypes (r114, r194, r262, r334, r347 and b2), along with two control strains (r21, r23) with typical phenotypes for *S. cerevisiae* and *S. uvarum* mitotypes, respectively, were subjected to whole genome sequencing and phenotyping.

DNA extraction, library preparation, and sequencing

For the unselected putative recombinants and their controls (r21, r23, b2, r334, r114, r194, r262, and r347), DNA was extracted using an mtDNA-enriching protocol (see

below). For other strains sequenced in this study, genomic DNA was extracted from 22°C YPD overnight cultures inoculated with cells pre-grown on YPGly plates (ZR Fungal/Bacterial DNA MicroPrep kit, Zymo Research).

mtDNA was enriched following a protocol adapted from (*50*) and (*26*). 50ml YPEG (1% yeast extract, 2% peptone, 2% ethanol, 2% glycerol) medium was inoculated with overnight YPD starter cultures, shaken at 300rpm at 22°C. The culture was collected at late-log phase (3,000g for 1 min) and the cell pellet was washed twice in 1ml sterile distilled water. The cells were then washed in buffer (1.2M Sorbitol, 50mM Tris pH 7.4, 50mM EDTA, 2% beta-mercaptoethanol) and centrifuged at 14,000 rpm for 3 minutes. The cell pellet was weighed, resuspended in Solution A (0.5M Sorbitol, 50mM Tris pH 7.4, 10mM EDTA, 2% beta-mercaptoethanol, 7ml/g wet weight cells) containing 0.2mg/ml Zymolyase (Zymo Research), and incubated at 37°C, 100 rpm for 45min for osmotic lysis. The suspension was then centrifuged at 4,000rpm for 10min. The supernatant was decanted to a new tube and centrifuged at 14,000 rpm for 15min, to get the crude mitochondrial pellet. The pellet was then incubated in DNase treatment solution [0.3M Sucrose, 5mM $MgCl_2$, 50mM Tris-HCl pH 8.0, 10mM $CaCl_2$, 100U/ml RQ1 Dnase (Promega), 500ul/g initial wet weight] at 37°C, 100 rpm for 30min to remove nuclear DNA. 0.5M EDTA (pH 8.0) was added to a final concentration of 0.2M to stop the reaction. The mitochondrial pellet was then washed three times by repeated cycles of centrifugation at 15,000 rpm for 10min and resuspension in 1ml solution A to remove DNase, and then resuspended in 400ul Solution B (100mM NaCl, 10mM EDTA, 50mM Tris pH 8) and incubated at room temperature for 30min for lysis. mtDNA was isolated from the solution by phenol-chloroform extraction and ethanol precipitation, followed by a clean-up with DNA clean and concentrator -5 kit (Zymo Research). Alternatively, two samples (r21and r262) were extracted with ZR Fungal/Bacterial DNA MicroPrep Kit (Zymo Research) by adding the Fungal/Bacterial DNA binding buffer to the lysed mitochondrial fraction and following the rest of the manufacturer protocol. The yield was typically 10-20ng/g wet weight cells and provided 10- to 100-fold enrichment of mitochondrial reads.

Paired-end libraries were prepared with Nextera DNA Library Preparation Kit (Illumina) with a modified protocol. Briefly, 3-5 ng DNA was used for each sample and the tagmentation reaction was performed at a ratio of 0.25ul tagmentation enzyme/ng DNA. The tagmented DNA was amplified by KAPA HiFi DNA polymerase for 13 cycles (72°C 3min; 98°C 5min; 98°C 10s, 63°C 30s, 72°C 30s for 13 cycles; 72°C 5min). The PCR reaction was then purified with AMPure Beads. Paired-end 2x150 Illumina sequencing was performed on a MiniSeq by the DNA Sequencing Innovation Lab in the Center for Genome Sciences and System Biology at Washington University. 96 recombinants generated in the second trial of the mitochondrial mutant crosses were subsequently re-sequenced on a NextSeq 500 at Duke Center for Genomic and Computational Biology for deeper coverage. The NextSeq reads and MiniSeq reads were combined in the analysis. The reads were deposited at the Sequence Read Archive under accession no. SRP155764.

Mitochondrial genome assembly

The *S. uvarum* mitochondrial genome was assembled from high-coverage sequencing of r23. Before assembly, we confirmed that it carried a non-recombinant *S. uvarum* mitochondrial genome by mapping the reads to CBS380 (*51*), an *S. eubayanus* × *S. uvarum* × *S. cerevisiae* hybrid that inherited the mitochondria from *S. uvarum*. To assemble the mitochondrial genome, reads were first cleaned with trimmomatic (*52*) to

remove adapters. They were then assembled using SPAdes assembler (*53*), included in the wrapper iWGS (*54*), to produce contigs. Contigs were scaffolded to produce the final assembly through comparison with the output assembly of MITObim (*55*). The assembly was annotated with Mfannot Tool (http://megasun.bch.umontreal.ca/RNAweasel/); *ORF1* (F-*Sce*III) annotation was added manually using Geneious R6 (*56*). The assembled r23 mitochondrial genome is 64,682 bp and has a total of 5,874 gapped bases (GenBank accession no. MH718505). Most gaps are in the intergenic regions, one gap is in *VAR1*, and 3 small gaps are in the introns of *COB*. The r23 mitochondrial genome is 99% identical to CBS380, based on BLAST results.

Read mapping and allele assignment of recombinants

Illumina reads were mapped to a reference that combined the mitochondrial genomes of *S. cerevisiae* (S288C-R64-2-1) and *S. uvarum* (r23 mitochondria assembled in this study), using end-to-end alignment in Bowtie 2 (*57*). Duplicated reads and reads with high secondary alignment scores (XS>=AS) or low mapping quality (MQ < 10) were filtered out. Using this method, reads from hybrids with non-recombinant *S. cerevisiae* or *S. uvarum* mtDNA were >99.9% correctly mapped to their reference genomes (49,496/49,504 for *S. cerevisiae*, 161,712/161,714 for *S. uvarum*). To characterize aneuploidy and the ratio of mitochondrial to nuclear reads, the reads were re-mapped to a reference file combining *S. cerevisiae* (S288C-R64-2-1) and *S. uvarum* (*42*) reference genomes, using the same method. Coverage of nucleotide positions and of chromosomes was generated by *samtools depth* and *samtools idxstats*, respectively.

For data visualization and identification of recombination breakpoints, we assigned allele identity for each nucleotide in orthologous regions in the two reference mitochondrial genomes. The total length of orthologous sequences is 16.5kb (nucmer alignment) and contains mostly coding and tRNA sequences. After removing sites with no coverage in control strains, 12.6k nucleotide positions were subjected to data visualization and allele calling. We called the allele identity of a given nucleotide position based on the ratio of reads that mapped to the *S. cerevisiae* reference allele to the total number of reads that mapped to the two orthologous alleles (rsc=sc/(sc+su)): rsc of 1 (or no lower than the non-recombinant *S. cerevisiae* mtDNA control) was called *S. cerevisiae*, rsc of 0 (or no higher than the non-recombinant *S. uvarum* mtDNA control) was called *S. uvarum*, rsc > 0 and < 1 were called mixed. Sites without coverage of either allele were treated as missing data. A relaxed threshold was used in data visualization to account for noise in read mapping (rsc >0.9 was called *S. cerevisiae*, labeled as "sc-90"; rsc <0.1 was called *S. uvarum*, labeled as "su-90"). Using this method, a total of 90 sequenced strains were confirmed to be recombinants.

For quantifying the effect size of *S. cerevisiae* alleles, we counted the number of reads mapped to each protein-coding gene, tRNA and rRNA by htseq-count. For each gene, we tested the allele effect across 90 recombinants using a linear model: *phenotype ~ allele + petite*, where *allele* is the ratio of *S. cerevisiae* reads for a given gene and *petite* is the empirically determined petite rates (see below). Because we used the ratio of *S. cerevisiae* reads to represent allele identity, the model does not assume dominance; a heterozygous individual (i.e. read ratio = 0.5) should have an intermediate phenotype. P-values were extracted from the models and adjusted by the false discovery rate (Benjamini & Hochberg method) to correct for multiple comparisons. While the p-value for the *petite* term is significant in some models, its effect was always estimated to be positive. Because high petite rates should lead to small colonies, we do not consider petite rate to significantly contribute to the phenotype. Additionally, aneuploidy and mtDNA copy

number variation were present in several recombinants, but the addition of the two variables to the model did not change the effect size and significance of the *allele* term (*phenotype ~ allele + petite+ aneuploidy + copy*, where *aneuploidy* is a binary variable indicating presence/absence of chromosomal duplication and *copy* is the ratio of mitochondrial to nuclear reads). See Data S2 for all data used in the models.

The unselected putative recombinants were sequenced to high coverage, so we generated contigs and assemblies as in "Mitochondrial genome assembly". The contigs were mapped to *S. cerevisiae* (r21) and *S. uvarum* (r23/CBS380/CBS7001) assemblies in Geneious R6 to identify the breakpoints. For the recombinants of lower quality assemblies (r194, r347, and b2), the contigs were mapped to the best recombinant assembly r114 to improve recombinant construction. Results were confirmed by retaining the Illumina reads from the mitochondrial genome, using both reference mitochondrial genomes as baits in HybPiper (*58*) and mapping them to the reference mitochondrial genomes using Geneious R6.

Recombinant phenotypes

Recombinant strains were first grown on YPGly plates to enrich for respiring cells, then in liquid YPD shaken at room temperature overnight. The overnight culture was diluted $1{:}10^5$, spread on YPD and YPGly plates and incubated at 22°C, 37°C, or 4°C. Pictures of plates were taken on the 5^{th} day for 22°C and 37°C YPD plates, on the 6^{th} day for 22°C and 37°C YPGly plates and on the 68^{th} day for 4°C YPD and YPGly plates. Colony sizes on YPGly plates were acquired by the *Analyze Particles* function in ImageJ (*49*). Non-single colonies were filtered out both by manually marking problematic colonies during analysis and by roundness threshold (roundness > 0.8 for non-petite colonies). For each strain, sizes of all the non-petite colonies (colony size > 200 units) were averaged; if no cells were respiring at a given condition, the average of all the (micro)colonies was used instead. Petite rates of the overnight cultures were recorded by counting big/small colonies on 22°C YPD and normal/micro colonies on 22°C YPGly plates, and the two values were averaged. Control strains carrying wild-type *S. cerevisiae* or *S. uvarum* mtDNA in the background of D273-10B × CBS7001 were phenotyped in parallel.

Initially the ~90 strains were phenotyped in three batches. We accounted for the batch effect for the 37°C data by picking 3-4 strains from each batch and repeating the phenotyping process on the same day at 37°C. Linear models between old data and new data were generated for each batch separately and were used to adjust for an overall batch effect. The 22°C colony sizes were not adjusted.

Mitochondrial allele replacement

Mitochondrial transformation was performed as previously described (*25*) (Fig. S6). Intronless mitochondrial alleles were synthesized by Biomatik. The alleles were Gibson-assembled into an *ARG8m*-baring pBluescript plasmid, such that the mitochondrial allele is flanked by 69 bp and 1113 bp *ARG8m* sequences at its 5' and 3' end, respectively (Fig. S6C). Sequences of the assembled plasmid were confirmed by Sanger sequencing.

Mitochondrial knockout strains were first transformed with P_{GAL}*-HO* to switch mating types and validated by mating type PCR. In these strains, the target gene was replaced with *ARG8m*, so our constructs carrying the allele of interest can integrate into their endogenous loci by homologous recombination with *ARG8m* (Fig. S6C).

We bombarded the mitochondrial plasmid and pRS315 (CEN plasmid carrying *LEU2*) into *S. cerevisiae* strain DFS160 (*MATα ade2-101 leu2Δ ura3-52 arg8Δ::URA3*

kar1-1, *rho*^{0}) (*45*) using a biolistic PDS-1000/He particle delivery system (Bio-Rad) and selected for Leu+ colonies on MM plates. The colonies were replica-mated to the mitochondrial knockout strains at 30°C for 2 days. The mating mixtures were replica-plated to YPGly plates and incubated at 30°C. YPGly+ colonies were streaked on YPD and mating types were determined by PCR. We also isolated the DFS160-derived parent strains that gave rise to the YPGly+ colonies from the master plates. For *S. cerevisiae* *COX1* and *COB* alleles, the parent strains were re-mated to the knockout strains for confirmation.

The YPGly+ colonies carry a mitochondrial genome with the allele of interest integrated at their endogenous loci. Because of the *kar1-1* mutation in DFS160, we were able to isolate YPGly+ colonies that are diploid, *MAT***a** haploid, or *MAT*α haploid. We crossed the *MAT***a** transformant (D273-10B background) to an *S. uvarum* rho^{0} strain (YJF2760). The hybrid strain and the diploid *S. cerevisiae* strains directly obtained from the mitochondrial transformation were phenotyped at room temperature, 37°C, and 4°C on YPD and YPGly by spot dilution assays. The allele identity of all the phenotyped strains was confirmed by PCR and restriction digest.

H2: Supplementary Materials

Supplementary Text
Fig. S1. Reciprocal hemizygosity test of *HFA1* and *CUP2*.
Fig. S2. Fermentative and respiratory growth of interspecific hybrids with reciprocal mitotypes at different temperatures.
Fig. S3. Rescue of *S. cerevisiae* (sc) mitochondrial knockouts by recombination with *S. uvarum* (su) mitotypes.
Fig. S4. Recombinant genotypes and examples of recombination breakpoints.
Fig. S5. High petite rate of *S. uvarum* mitotype and its association with *ORF1*.
Fig. S6. Procedure for mitochondrial allele replacement.
Fig. S7. Background-dependent allele effects of *COX1*.
Table S1. Aneuploidy in the recombinants.
Table S2. (separate file) Strains used in this study.
Data file S1. (separate file) Results of non-complementation screen.
Data file S2. (separate file) Recombinant strain genotypes and phenotypes. Allele, petite rate, aneuploidy, and mito/nuclear read ratio of the 90 mitochondrial recombinants used in the linear model.

References and Notes

1. H. Orr, J. Coyne, The genetics of adaptation: a reassessment. *Am. Nat.* **140**, 725–742 (1992).
2. H. A. Orr, The genetics of species differences. *Trends Ecol. Evol.* **16**, 343–350 (2001).
3. A. Hagman, T. Säll, C. Compagno, J. Piskur, Yeast "Make-Accumulate-Consume" Life Strategy Evolved as a Multi-Step Process That Predates the Whole Genome Duplication. *PLoS One*. **8**, e68734 (2013).
4. P. Gonçalves, E. Valério, C. Correia, J. M. G. C. F. de Almeida, J. P. Sampaio, Evidence for divergent evolution of growth temperature preference in sympatric Saccharomyces species. *PLoS One*. **6**, e20739 (2011).
5. Z. Salvadó, F. N. Arroyo-López, J. M. Guillamón, G. Salazar, A. Querol, E. Barrio, Temperature adaptation markedly determines evolution within the genus Saccharomyces.

Appl. Environ. Microbiol. **77**, 2292–302 (2011).
6. C. M. Paget, J. M. Schwartz, D. Delneri, Environmental systems biology of cold-tolerant phenotype in Saccharomyces species adapted to grow at different temperatures. *Mol. Ecol.* **23**, 5241–5257 (2014).
7. C. V. Weiss, J. I. Roop, R. K. Hackley, J. N. Chuong, I. V Grigoriev, A. P. Arkin, J. M. Skerker, R. B. Brem, Genetic dissection of interspecific differences in yeast thermotolerance. *Nat. Genet.* (2018), doi:10.1038/s41588-018-0243-4.
8. Y. Kawahara, T. Imanishi, A genome-wide survey of changes in protein evolutionary rates across four closely related species of Saccharomyces sensu stricto group. *BMC Evol. Biol.* **7**, 1–13 (2007).
9. R. H. Waterston *et al.*, Initial sequencing and comparative analysis of the mouse genome. *Nature*. **420**, 520–562 (2002).
10. H.-Y. Lee, J.-Y. Chou, L. Cheong, N.-H. Chang, S.-Y. Yang, J.-Y. Leu, Incompatibility of nuclear and mitochondrial genomes causes hybrid sterility between two yeast species. *Cell*. **135**, 1065–73 (2008).
11. J.-Y. Chou, Y.-S. Hung, K.-H. Lin, H.-Y. Lee, J.-Y. Leu, Multiple molecular mechanisms cause reproductive isolation between three yeast species. *PLoS Biol.* **8**, e1000432 (2010).
12. N. Hunter, S. R. Chambers, E. J. Louis, R. H. Borts, The mismatch repair system contributes to meiotic sterility in an interspecific yeast hybrid. *EMBO J.* **15**, 1726–1733 (1996).
13. G. Liti, D. B. H. Barton, E. J. Louis, Sequence diversity, reproductive isolation and species concepts in Saccharomyces. *Genetics*. **174**, 839–50 (2006).
14. D. Delneri, I. Colson, S. Grammenoudi, I. N. Roberts, E. J. Louis, S. G. Oliver, Engineering evolution to study speciation in yeasts. *Nature*. **422**, 68–72 (2003).
15. G. Fischer, C. Neuvéglise, P. Durrens, C. Gaillardin, B. Dujon, Evolution of gene order in the genomes of two related yeast species. *Genome Res.* **11**, 2009–19 (2001).
16. J. F. Wolters, G. Charron, A. Gaspary, C. R. Landry, A. C. Fiumera, H. L. Fiumera, Mitochondrial Recombination Reveals Mito–Mito Epistasis in Yeast. *Genetics*. **209**, 307–319 (2018).
17. S. Paliwal, A. C. Fiumera, H. L. Fiumera, Mitochondrial-nuclear epistasis contributes to phenotypic variation and coadaptation in natural isolates of Saccharomyces cerevisiae. *Genetics*. **198**, 1251–65 (2014).
18. J. B. Leducq, M. Henault, G. Charron, L. Nielly-Thibault, Y. Terrat, H. L. Fiumera, B. J. Shapiro, C. R. Landry, Mitochondrial recombination and introgression during speciation by hybridization. *Mol. Biol. Evol.* **34**, 1947–1959 (2017).
19. L. M. Steinmetz, H. Sinha, D. R. Richards, J. I. Spiegelman, P. J. Oefner, J. H. McCusker, R. W. Davis, Dissecting the architecture of a quantitative trait locus in yeast. *Nature*. **416**, 326–30 (2002).
20. C. Buchman, P. Skroch, J. Welch, S. Fogel, M. Karin, The CUP2 gene product, regulator of yeast metallothionein expression, is a copper-activated DNA-binding protein. *Mol. Cell. Biol.* **9**, 4091–4095 (1989).
21. W. Albertin, T. da Silva, M. Rigoulet, B. Salin, I. Masneuf-Pomarede, D. de Vienne, D. Sicard, M. Bely, P. Marullo, The mitochondrial genome impacts respiration but not fermentation in interspecific Saccharomyces hybrids. *PLoS One*. **8**, e75121 (2013).
22. U. Hoja, S. Marthol, J. Hofmann, S. Stegner, R. Schulz, S. Meier, E. Greiner, E. Schweizer, HFA1 encoding an organelle-specific acetyl-CoA carboxylase controls mitochondrial fatty acid synthesis in Saccharomyces cerevisiae. *J. Biol. Chem.* **279**, 21779–21786 (2004).
23. E. P. Baker, D. Peris, R. V Moriarty, X. C. Li, J. C. Fay, C. T. Hittinger, Mitochondrial

DNA and temperature tolerance in lager yeasts, 1–18 (2018).
24. D. Peris, A. Arias, S. Orlić, C. Belloch, L. Pérez-Través, A. Querol, E. Barrio, Mitochondrial introgression suggests extensive ancestral hybridization events among Saccharomyces species. *Mol. Phylogenet. Evol.* **108**, 49–60 (2017).
25. N. Bonnefoy, T. D. Fox, in *Methods in Cell Biology* (2001; http://linkinghub.elsevier.com/retrieve/pii/S0091679X01650222), vol. 80, pp. 381–396.
26. J. F. Wolters, K. Chiu, H. L. Fiumera, Population structure of mitochondrial genomes in Saccharomyces cerevisiae. *BMC Genomics*. **16**, 451 (2015).
27. M. Spirek, S. Polakova, K. Jatzova, P. Sulo, Post-zygotic sterility and cytonuclear compatibility limits in S. cerevisiae xenomitochondrial cybrids. *Front. Genet.* **5**, 1–15 (2015).
28. C. Auesukaree, A. Damnernsawad, M. Kruatrachue, P. Pokethitiyook, C. Boonchird, Y. Kaneko, S. Harashima, Genome-wide identification of genes involved in tolerance to various environmental stresses in Saccharomyces cerevisiae. *J. Appl. Genet.* **50**, 301–10 (2009).
29. A. J. Kastaniotis, K. J. Autio, J. M. Kerätär, G. Monteuuis, A. M. Mäkelä, R. R. Nair, L. P. Pietikäinen, A. Shvetsova, Z. Chen, J. K. Hiltunen, Mitochondrial fatty acid synthesis, fatty acids and mitochondrial physiology. *Biochim. Biophys. Acta - Mol. Cell Biol. Lipids*. **1862**, 39–48 (2017).
30. F. Suomi, K. E. Menger, G. Monteuuis, U. Naumann, V. A. S. Kursu, A. Shvetsova, A. J. Kastaniotis, Expression and Evolution of the Non-Canonically Translated Yeast Mitochondrial Acetyl-CoA Carboxylase Hfa1p. *PLoS One*. **9**, e114738 (2014).
31. F.-N. Vögtle, J. M. Burkhart, H. Gonczarowska-Jorge, C. Kücükköse, A. A. Taskin, D. Kopczynski, R. Ahrends, D. Mossmann, A. Sickmann, R. P. Zahedi, C. Meisinger, Landscape of submitochondrial protein distribution. *Nat. Commun.* **8**, 290 (2017).
32. H. Jhuang, H. Lee, J. Leu, Mitochondrial–nuclear co-evolution leads to hybrid incompatibility through pentatricopeptide repeat proteins. *EMBO Rep.* **18**, 87–101 (2017).
33. E. M. Piatkowska, S. Naseeb, D. Knight, D. Delneri, Chimeric Protein Complexes in Hybrid Species Generate Novel Phenotypes. *PLoS Genet.* **9** (2013), doi:10.1371/journal.pgen.1003836.
34. P. Sulo, D. Szabóová, P. Bielik, S. Poláková, K. Šoltys, K. Jatzová, T. Szemes, The evolutionary history of Saccharomyces species inferred from completed mitochondrial genomes and revision in the 'yeast mitochondrial genetic code.' *DNA Res.* **24**, 571–583 (2017).
35. M. Kellis, N. Patterson, M. Endrizzi, B. Birren, E. S. Lander, Sequencing and comparison of yeast species to identify genes and regulatory elements. *Nature*. **423**, 241–54 (2003).
36. R. S. Burton, F. S. Barreto, A disproportionate role for mtDNA in Dobzhansky-Muller incompatibilities? *Mol. Ecol.* **21**, 4942–57 (2012).
37. L. Solieri, O. Antunez, J. E. Perez-Ortin, E. Barrio, P. Giudici, Mitochondrial inheritance and fermentative: oxidative balance in hybrids between Saccharomyces cerevisiae and Saccharomyces uvarum. *Yeast*. **25**, 485–500 (2008).
38. C. Picazo, E. Gamero-Sandemetrio, H. Orozco, W. Albertin, P. Marullo, E. Matallana, A. Aranda, Mitochondria inheritance is a key factor for tolerance to dehydration in wine yeast production. *Lett. Appl. Microbiol.* **60**, 217–222 (2014).
39. E. I. Zubko, M. K. Zubko, Deficiencies in mitochondrial DNA compromise the survival of yeast cells at critically high temperatures. *Microbiol. Res.* **169**, 185–95 (2014).
40. M. K. Vorachek-Warren, J. H. McCusker, DsdA (D-serine deaminase): a new heterologous MX cassette for gene disruption and selection in Saccharomyces cerevisiae. *Yeast*. **21**, 163–71 (2004).

41. R. D. Gietz, R. H. Schiestl, A. R. Willems, R. A. Woods, Studies on the transformation of intact yeast cells by the LiAc/SS-DNA/PEG procedure. *Yeast*. **11**, 355–360 (1995).
42. D. R. Scannell, O. A. Zill, A. Rokas, C. Payen, M. J. Dunham, M. B. Eisen, J. Rine, M. Johnston, C. T. Hittinger, The Awesome Power of Yeast Evolutionary Genetics: New Genome Sequences and Strain Resources for the Saccharomyces sensu stricto Genus. *G3 (Bethesda).* **1**, 11–25 (2011).
43. X. Perez-Martinez, S. A. Broadley, T. D. Fox, Mss51p promotes mitochondrial Cox1p synthesis and interacts with newly synthesized Cox1p. *EMBO J.* **22**, 5951–61 (2003).
44. N. Bonnefoy, T. D. Fox, In vivo analysis of mutated initiation codons in the mitochondrial COX2 gene of Saccharomyces cerevisiae fused to the reporter gene ARG8mreveals lack of downstream reinitiation. *Mol. Gen. Genet.* **262**, 1036–1046 (2000).
45. D. F. Steele, C. A. Butler, T. D. Fox, Expression of a recoded nuclear gene inserted into yeast mitochondrial DNA is limited by mRNA-specific translational activation. *Proc. Natl. Acad. Sci. U. S. A.* **93**, 5253–7 (1996).
46. M. G. Ding, C. A. Butler, S. A. Saracco, T. D. Fox, F. Godard, J. di Rago, B. L. Trumpower, in *Methods in Enzymology* (2009; http://linkinghub.elsevier.com/retrieve/pii/S0076687908044273), vol. 456, pp. 491–506.
47. M. Rak, E. Tetaud, F. Godard, I. Sagot, B. Salin, S. Duvezin-Caubet, P. P. Slonimski, J. Rytka, J. P. Di Rago, Yeast cells lacking the mitochondrial gene encoding the ATP synthase subunit 6 exhibit a selective loss of complex IV and unusual mitochondrial morphology. *J. Biol. Chem.* **282**, 10853–10864 (2007).
48. M. Rak, A. Tzagoloff, F1-dependent translation of mitochondrially encoded Atp6p and Atp8p subunits of yeast ATP synthase. *Proc. Natl. Acad. Sci. U. S. A.* **106**, 18509–14 (2009).
49. W. Rasband, ImageJ, U. S. National Institutes of Health, Bethesda, Maryland, USA, https://imagej.nih.gov/ij/, 1997-2016.
50. E. S. Fritsch, C. D. Chabbert, B. Klaus, L. M. Steinmetz, A Genome-Wide Map of Mitochondrial DNA Recombination in Yeast. *Genetics*. **198**, 755–771 (2014).
51. M. Okuno, R. Kajitani, R. Ryusui, H. Morimoto, Y. Kodama, T. Itoh, Next-generation sequencing analysis of lager brewing yeast strains reveals the evolutionary history of interspecies hybridization. *DNA Res.* **23**, 67–80 (2016).
52. A. M. Bolger, M. Lohse, B. Usadel, Trimmomatic: a flexible trimmer for Illumina sequence data. *Bioinformatics*. **30**, 2114–2120 (2014).
53. A. Bankevich, S. Nurk, D. Antipov, A. A. Gurevich, M. Dvorkin, A. S. Kulikov, V. M. Lesin, S. I. Nikolenko, S. Pham, A. D. Prjibelski, A. V. Pyshkin, A. V. Sirotkin, N. Vyahhi, G. Tesler, M. A. Alekseyev, P. A. Pevzner, SPAdes: A New Genome Assembly Algorithm and Its Applications to Single-Cell Sequencing. *J. Comput. Biol.* **19**, 455–477 (2012).
54. X. Zhou, D. Peris, J. Kominek, C. P. Kurtzman, C. T. Hittinger, A. Rokas, in silico Whole Genome Sequencer and Analyzer (iWGS): a Computational Pipeline to Guide the Design and Analysis of de novo Genome Sequencing Studies. *G3*. **6**, 3655–3662 (2016).
55. C. Hahn, L. Bachmann, B. Chevreux, Reconstructing mitochondrial genomes directly from genomic next-generation sequencing reads--a baiting and iterative mapping approach. *Nucleic Acids Res.* **41**, e129–e129 (2013).
56. M. Kearse, R. Moir, A. Wilson, S. Stones-Havas, M. Cheung, S. Sturrock, S. Buxton, A. Cooper, S. Markowitz, C. Duran, T. Thierer, B. Ashton, P. Meintjes, A. Drummond, Geneious Basic: An integrated and extendable desktop software platform for the organization and analysis of sequence data. *Bioinformatics*. **28**, 1647–1649 (2012).
57. B. Langmead, S. L. Salzberg, Fast gapped-read alignment with Bowtie 2. *Nat Methods*. **9**, 357–359 (2012).

58. M. G. Johnson, E. M. Gardner, Y. Liu, R. Medina, B. Goffinet, A. J. Shaw, N. J. C. Zerega, N. J. Wickett, HybPiper: Extracting Coding Sequence and Introns for Phylogenetics from High-Throughput Sequencing Reads Using Target Enrichment. *Appl. Plant Sci.* **4**, 1600016 (2016).
59. L. N. Dimitrov, R. B. Brem, L. Kruglyak, D. E. Gottschling, Polymorphisms in Multiple Genes Contribute to the Spontaneous Mitochondrial Genome Instability of Saccharomyces cerevisiae S288C Strains. *Genetics*. **183**, 365–383 (2009).
60. R. Bordonné, G. Dirheimer, R. P. Martin, Expression of the oxi1 and maturase-related RF1 genes in yeast mitochondria. *Curr. Genet.* **13**, 227–233 (1988).
61. A. Jacquier, B. Dujon, An intron-encoded protein is active in a gene conversion process that spreads an intron into a mitochondrial gene. *Cell*. **41**, 383–394 (1985).
62. D. Peris *et al.*, Hybridization and adaptive evolution of diverse Saccharomyces species for cellulosic biofuel production. *Biotechnol. Biofuels*. **10**, 78 (2017).
63. A. Burt, V. Koufopanou, Homing endonuclease genes: the rise and fall and rise again of a selfish element. *Curr. Opin. Genet. Dev.* **14**, 609–615 (2004).

Acknowledgments

General: We thank Tom D. Fox, Alexander Tzagoloff, Javier Alonso del Real Arias and Amparo Querol for sharing strains. We thank members of Fay lab for comments and experimental assistance.

Funding: This work was supported by a National Institutes of Health grant (GM080669) to J.C.F. Additional support to C.T.H. was provided by the USDA National Institute of Food and Agriculture (Hatch project 1003258), the National Science Foundation (DEB-1253634), and the DOE Great Lakes Bioenergy Research Center (DOE BER Office of Science DE-SC0018409 and DE-FC02-07ER64494 to Timothy J. Donohue). C.T.H. is a Pew Scholar in the Biomedical Sciences and a Vilas Faculty Early Career Investigator, supported by the Pew Charitable Trusts and the Vilas Trust Estate, respectively. D.P. is a Marie Sklodowska-Curie fellow of the European Union's Horizon 2020 research and innovation programme, grant agreement No. 747775.

Author contributions: Conceptualization, X.C.L. and J.C.F.; Methodology, X.C.L., E.A.S. and J.C.F.; Investigation, X.C.L.; Writing – original draft: X.C.L. and J.C.F.; Writing – review & editing: D.P. and C.T.H.; Funding acquisition: J.C.F.; Resources, D.P., C.T.H. and E.A.S.; Supervision: C.T.H. and J.C.F.

Competing interests: Authors declare no competing interests.

Data and materials availability: The Illumina reads were deposited at the Sequence Read Archive under accession no. SRP155764. The mitochondrial genome assembly of *S. uvarum* (r23) was deposited at GenBank under accession no. MH718505. Other data, code, and materials are available upon request.

Figures and Tables

Fig. 1

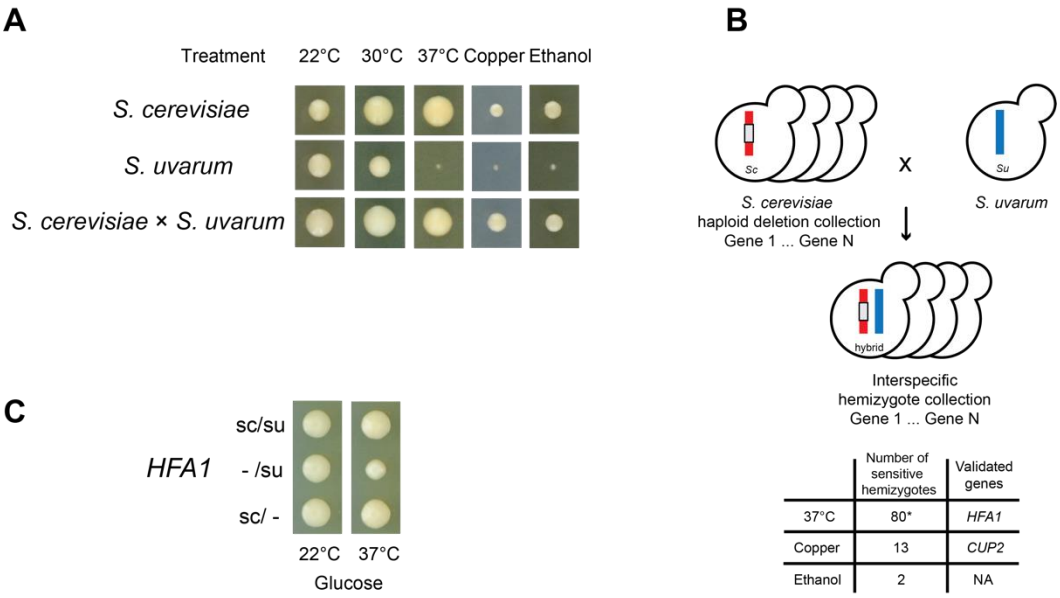

831

832 **Fig. 1. A non-complementation screen identified genes underlying phenotypic**
833 **divergence between *S. cerevisiae* and *S. uvarum*.** (**A**) *S. cerevisiae* and *S. uvarum* differ
834 in heat (37°C), copper (0.5mM, 22°C), and ethanol (10%, 30°C) tolerance. The resistant *S.*
835 *cerevisiae* alleles are dominant, shown by the hybrid (*S. cerevisiae* × *S. uvarum*) compared
836 to *S. cerevisiae* (diploid, S288C background) and *S. uvarum* (diploid, CBS7001
837 background). Growth is after 3 days. (**B**) *S. cerevisiae* haploid deletion collection was
838 crossed to *S. uvarum* to construct an interspecies hemizygote collection. The number of
839 non-complementing genes is shown for each phenotype; the asterisk indicates that the
840 number includes strains carrying *S. uvarum* mtDNA. (**C**) *HFA1* hemizygote with only an
841 *S. cerevisiae* allele (sc/-) shows better 37°C growth than one with only an *S. uvarum* allele
842 (-/su). Growth is after 5 days. See Fig. S1B for quantification.

843

Fig. 2

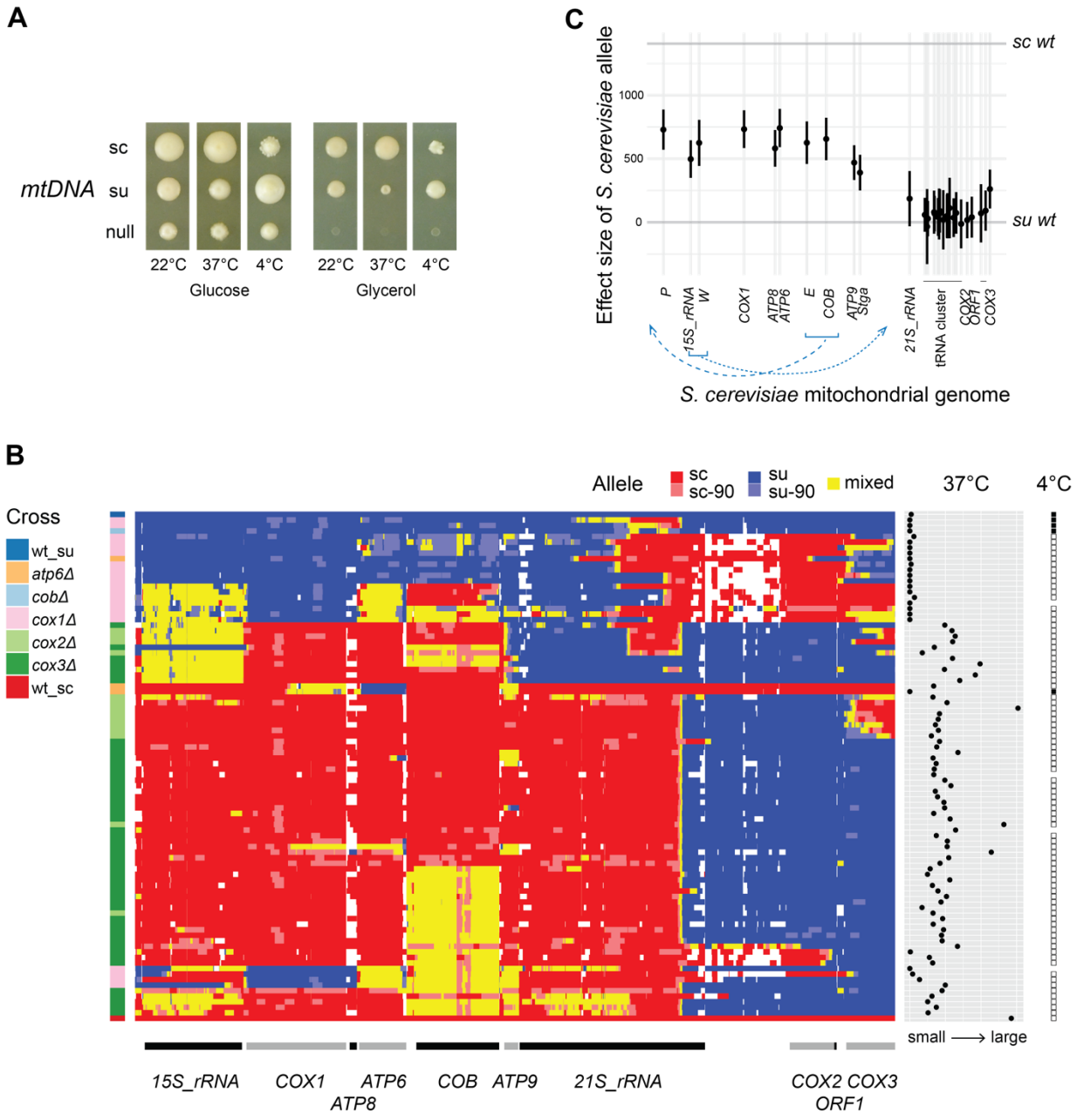

Fig. 2. Mitochondria-encoded genes affect divergence in heat and cold tolerance. (**A**) *S. cerevisiae* (sc) mtDNA confers heat tolerance while *S. uvarum* (su) mtDNA confers cold tolerance. (**B**) Recombinant strains (rows) derived from mutant crosses (left) are clustered by genotype (middle). Wild-type *S. cerevisiae* (wt_sc) and *S. uvarum* (wt_su) mitotype controls are at the bottom and the top, respectively. Allele identity is shown for 12.6k orthologous single nucleotide markers (sc and sc-90, *S. cerevisiae*; su and su-90, *S. uvarum*; mixed, heterozygous or chimeric; white, no data) in the *S. cerevisiae* gene order (bottom). 37°C growth is the average size of non-petite colonies on glycerol plates (right). The presence of 4°C glycerol growth is indicated by solid squares (far right). (**C**) Effect

size of *S. cerevisiae* alleles on 37°C growth on glycerol, with error bars representing 95% confidence intervals. The y-axis is rescaled such that 0 and the top horizontal line represent the phenotype of wild-type *S. uvarum* and *S. cerevisiae* mitotype, respectively. Selected tRNAs are labeled by their single letter amino acid code, while others are marked by a black bar (e.g. the tRNA cluster). Blue dashed lines indicate genome positions of *S. uvarum* genes compared to *S. cerevisiae*.

Fig. 3

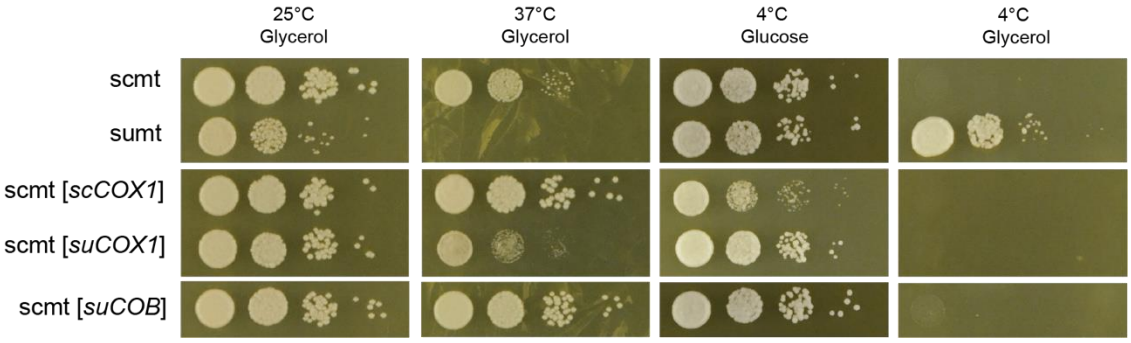

Fig. 3. *COX1* coding alleles affect growth at high and low temperature. Hybrids carrying allele replacements and two wild-type controls were plated with 1:10 serial dilution and incubated at indicated temperatures. Growth is after 4 days for 25°C and 37°C, 25 days for 4°C on glucose, 53 days for 4°C on glycerol. sc, *S. cerevisiae*; su, *S. uvarum*; mt, mtDNA. Alleles in the brackets were integrated into their endogenous position in *S. cerevisiae* mtDNA.

Supplementary Materials

Supplementary Text

High petite rate of *S. uvarum* mitotype and its association with *ORF1*

Saccharomyces yeast strains generate petites spontaneously at a rate of ~1%, and variants in nuclear genes can affect petite rates (*59*). We observed an extremely high petite rate in the hybrid with *S. uvarum* mitotype (48-61%, sometimes >90%), while the hybrid carrying *S. cerevisiae* mtDNA rarely generates petites (Fig. S5A). The high petite rate associated with *S. uvarum* mtDNA is only seen in the interspecific hybrid, but not pure strains *S. uvarum*, suggesting a dominant incompatibility in mtDNA inheritance between hybrid nuclear genomes and *S. uvarum* mtDNA. However, we were able to isolate a few *S. cerevisiae* and *S. uvarum* hybrids that carried mostly *S. uvarum* mitochondrial genes but did not exhibit a high petite rate. These strains arose at a frequency of 1%, so they are likely spontaneous recombinants. Whole genome sequencing showed that they all carry *S. cerevisiae ORF1*, but the rest of their mitochondrial genome is *S. uvarum* (Fig. S5C). This result suggests a strong link between *S. cerevisiae ORF1* and mtDNA inheritance. In the 90 recombinants generated from mutant crosses, we also observed a strong correlation between *S. cerevisiae ORF1* and low petite rates, although there were exceptions (Fig. S5B).

The possible inheritance phenotype adds to our understanding of the interesting biology of *ORF1*. *ORF1* (F-*Sce*III) was suggested to encode a free-standing homing endonuclease (*60*). The best-known homing endonuclease is I-*Sce*I (ω), which promotes its spread to homing-less mitochondrial genomes (*61*). *ORF1* (F-*Sce*III) has been proposed to mediate mitochondrial recombination based on the high frequency of interspecific mitochondrial recombinants at the start of *ORF1* in wild *Saccharomyces* species and in a synthetic hybrid of *S. cerevisiae* × *S. mikatae* (*24*, *62*). Although further work will be needed to demonstrate that *ORF1* affects mitochondrial inheritance, this activity would imply co-evolution between a selfish element and its host (*63*).

Fig. S1. Reciprocal hemizygosity test of *HFA1* and *CUP2*. (**A**) Hemizygotes with either the *S. cerevisiae* allele (sc/-) or *S. uvarum* allele (-/su) and a wild-type hybrid (sc/su) were compared under the same conditions as the non-complementation screen. Growth is after 5 days. (**B**) Heat or copper resistance was measured by colonies sizes normalized to control condition (22°C YPD), with error bars representing the standard deviation of 6 biological replicates. (**C**) *HFA1* hemizygotes differed in heat sensitivity on glucose but not glycerol medium. Cells were plated at 1:10 dilution. Growth is after 3 days.

Fig. S2. Fermentative and respiratory growth of interspecific hybrids with reciprocal mitotypes at different temperatures. Interspecific hybrids between *S. cerevisiae* (sc), *S. paradoxus* (sp), *S. kudriavzevii* (sk), and *S. uvarum* (su) with either parental mitotype (ρ^{p1} or ρ^{p2}) or no mtDNA (ρ^{o}) were grown on YPD and YPGly plates for 5 days (22°C and 37°C) or 124 days (4°C). Growth of parent species and their petites are shown for comparison. The 4°C images of *S. cerevisiae* × *S. kudriavzevii* hybrid with *S. cerevisiae* mtDNA (sc × sk ρ^{p1}) were replaced with images from a biological replicate plated in the same configuration because the original colony was contaminated.

Fig. S3. Rescue of *S. cerevisiae* (sc) mitochondrial knockouts by recombination with *S. uvarum* (su) mitotypes. Upon crossing *S. cerevisiae* with *S. uvarum*, hybrids have unstable heteroplasmy; parental types do not grow at 37°C on glycerol, but recombinants can rescue the *S. cerevisiae* deficiency and the *S. uvarum* temperature sensitivity.

Fig. S4. Recombinant genotypes and examples of recombination breakpoints. (**A**) Recombinants were manually classified into 11 genotype groups and breakpoints for 8 representatives were identified by manual inspection. Strains were labeled by the trials ("f" for initial trial and "S" for second trial) and mutant crosses in which they were generated. Phenotype panels are shown as in Fig. 2B, with the addition of 22°C colony sizes. (**B**) Representative recombinant genomes are shown. Outer circles represent the reference mitochondrial genomes (red for *S. cerevisiae*, blue for *S. uvarum*) and inner circles show coverage of a given recombinant. Note *15S rRNA* and *COB* are at different positions in the two reference genomes.

Fig. S5. High petite rate of *S. uvarum* mitotype and its association with *ORF1*. (**A**) Petite rate in a 22°C overnight culture is high for the hybrid with a *S. uvarum* mitotype (blue circle), while the hybrid with a *S. cerevisiae* mitotype (red circle) rarely generates petites (dotted circle). (**B**) Petite rates associate with *ORF1* alleles in 90 recombinants generated by knockout crosses. sc, *S. cerevisiae*; su, *S. uvarum*. (**C**) Four spontaneous recombinants carrying *S. cerevisiae ORF1* showed low petite rates; the rest of their mitochondrial genome is *S. uvarum*.

Fig. S6. Procedure for mitochondrial allele replacement. (**A**) Biolistic transformation of the mitochondrial construct with a *LEU2* plasmid. (**B**) Leu+ colonies were mated to *S. cerevisiae* mitochondrial knockouts. (**C**) The allele of interest was integrated into the mitochondrial genome via homologous recombination. (**D**) Integrated alleles were

selected by rescue of respiration. (**E**) *MAT***a** mitochondrial genome transformants were crossed to *S. uvarum*.

Fig. S7. Background-dependent allele effects of *COX1*. *S. cerevisiae* diploids and hybrids carrying allele replacements and two wild-type controls were plated with 1:10 serial dilution and incubated at indicated temperatures. Growth is after 4 days for 25°C and 37°C, 25 days for 4°C on glucose, and 53 days for 4°C on glycerol. sc, *S. cerevisiae*; su, *S. uvarum*; mt, mtDNA. Alleles in the brackets were integrated into their endogenous loci in *S. cerevisiae* mtDNA.

Table S1. Aneuploidy in the recombinants.

Strain	Increased 37°C growth compared to similar genotypes?	Cross	Duplicated chromosome	Mitochondrial interacting genes carried on the chromosome[1]	Reference
S29	Yes	*cox3*Δ	*S. cerevisiae* chrIX	*MRS1*	(*11*)
S53	No	*cox3*Δ	*S. cerevisiae* chrV	*MRX1*	(*32*)
S54	No	*cox3*Δ	*S. cerevisiae* chrIX	*MRS1*	(*11*)
S61	Yes	*cox3*Δ	*S. cerevisiae* chrIX	*MRS1*	(*11*)
S97	Yes	*cox1*Δ	*S. uvarum* chr10	*PET309*	(*32*)

[1] Only genes with known incompatibilities were listed.

External files:

Table S2. Strains used in this study.
Data file S1. Results of non-complementation screen.
Data file S2. Recombinant strain genotypes and phenotypes. Allele, petite rate, aneuploidy, and mito/nuclear read ratio of the 90 mitochondrial recombinants used in the linear model.